

Smectic vortex glass

Leo Radzihovsky ^{*}

Department of Physics and Center for Theory of Quantum Matter, University of Colorado, Boulder, Colorado 80309, USA



(Received 11 May 2021; accepted 15 July 2021; published 27 July 2021)

We show that in type-II superconductors a magnetic field applied transversely to correlated columnar disorder drives a phase transition to a distinct “smectic” vortex glass (SmVG) state. SmVG is characterized by an infinitely anisotropic electrical transport, resistive (dissipationless) for current perpendicular to (along) columnar defects. Its positional order is also quite unusual, long-ranged with true Bragg peaks along columnar defects and logarithmically rough vortex lattice distortions with quasi-Bragg peaks transverse to columnar defects. For low temperatures and sufficiently weak columnar-only disorder, SmVG is a true topologically ordered “Bragg glass,” characterized by a vanishing dislocation density. At sufficiently long scales the residual ever-present point disorder converts this state to a more standard but highly anisotropic vortex glass.

DOI: [10.1103/PhysRevB.104.024510](https://doi.org/10.1103/PhysRevB.104.024510)

I. INTRODUCTION

A. Background and motivation

The discovery of high-temperature superconductors, now more than 30 years ago, in parallel with a search for the microscopic “mechanism” (that continues to date) generated vigorous studies of vortex states of matter in the presence of thermal fluctuations, pinning disorder and electrical (“super”) current in and out of equilibrium [1–6], predicting and finding a rich magnetic field (H)–temperature (T) phase diagram of these type-II superconductors [7].

In contrast to a mean-field picture, thermal fluctuations drive a first-order melting of a vortex lattice over a large portion of the phase diagram into a resistive (though highly diamagnetic) vortex liquid [8–11].

In the low-temperature vortex solid state, arbitrarily weak point pinning disorder, on sufficiently long scale [12,13], always disrupts translational order of the vortex lattice. Supported by experimental observations [14], it was argued [3,15–17] that the resulting vortex glass state is characterized by an Edwards-Anderson [18] order parameter, with vortices collectively pinned, and thereby exhibiting a vanishing linear mobility, implying a zero linear resistivity of the vortex glass state [3]. For weak disorder, a distinct topologically ordered vortex Bragg glass, characterized by a vanishing density of unpaired dislocations and concomitant power-law decay of crystalline order, was also proposed [19], supported by further analytical [20–22] and numerical [23,24] analyses and by neutron scattering experiments [25].

Introduction (via heavy-ion irradiation) of columnar pinning defects significantly enhances pinning [26], and for a magnetic field along columnar defects was predicted to lead to an *anisotropic* vortex glass dubbed “Bose glass” [27,28] because of its mathematical connection to interacting two-

dimensional (2D) quantum bosons pinned by a quenched (time-independent) random 2D potential [29].

One key feature of the vortex Bose glass that qualitatively distinguishes it from the corresponding isotropic vortex glass is the existence of the “transverse” Meissner effect [28], namely a vanishing response to a field $H_{\perp} < H_{\perp}^{c1}$, applied transversely to columnar defects. This expulsion of the transverse flux density, B_{\perp} , which has received considerable experimental [30] and simulation [31] support, corresponds to an effectively divergent tilt modulus [28,32] inside this anisotropic vortex glass, which in the quantum correspondence maps onto a vanishing superfluid density in the Bose glass phase. A detailed theoretical description of the transverse Meissner effect (as well as other properties of the phase) has been predominantly limited to noninteracting vortex lines [28,33], supported by variable-range hopping [34] scaling theories [28,31,33,35], analysis in reduced planar geometry [36,37], and simulations [31,38].

As illustrated in Fig. 1(c), vortex Bose glass is thus confined to the low-temperature and low-transverse-magnetic-field part of the phase diagram [28]. To date, it has been tacitly assumed that beyond the critical value H_{\perp}^{c1} of the transverse field, the tilted state is a vortex liquid or crystal (a conventional vortex glass in the presence of residual point disorder [33]) with a finite resistivity and a finite tilt modulus, qualitatively the same vortex phase appearing above melting transition at T_g . Our goal here is to explore and characterize a highly tilted vortex geometry illustrated in Fig. 1(a), which, in the absence of point disorder at large tilting angle ($\sim \pi/2$), $H_{\perp} \gg H_{\perp}^{c1}$, we show is a qualitatively distinct vortex glass phase, which we dub as “smectic” vortex glass (SmVG). In fact, dating almost 20 years back, this regime has been explored experimentally [39], finding interesting anomalous behavior in the magnetic ac susceptometry and electrical transport, and motivating our theoretical study, which has taken this long to formalize.

The rest of the paper is organized as follows. We conclude the Introduction with a summary of our main results. In Sec. II we introduce an elastic model to describe a vortex array,

^{*}radzihov@colorado.edu

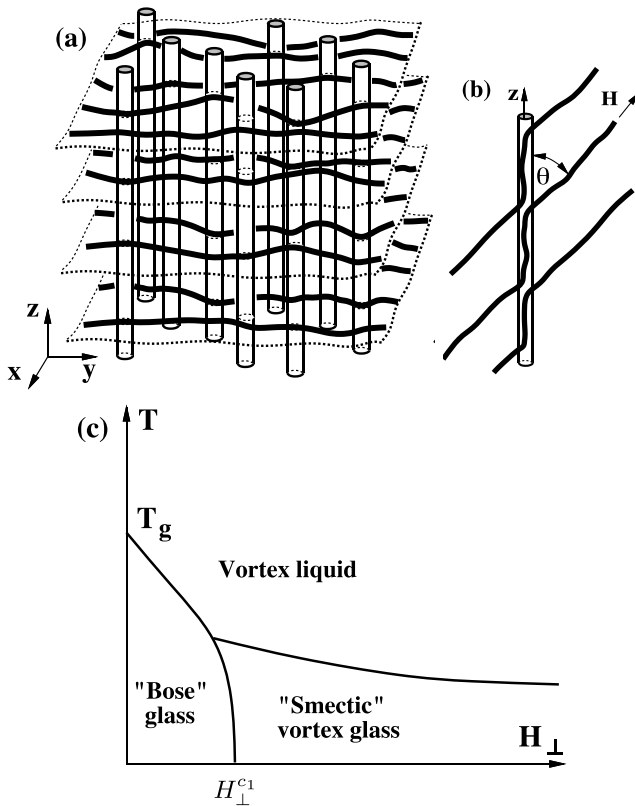


FIG. 1. (a) Illustration of the *transverse* magnetic field geometry in a positionally random array of parallel columnar defects, leading to the “smectic vortex glass” (SmVG) phase in (c). (b) Vortex lines’ tilt response to an applied field, applied transversely to a columnar defect. (c) A schematic phase diagram, illustrating a transverse Meissner effect up to field $H_{\perp}^{c1}(T)$, at which at low T a fully superconducting “Bose glass” undergoes a transition to a SmVG.

tilted at a large angle relative to the random forest of parallel columnar defects. Because pinning disorder does not couple to displacements along columnar defects, in Sec. III we reduce the system to an effective scalar model for a transverse-only distortion characterized by long-range elasticity, resembling an effective planar vortex glass model [15]. We analyze this model within and beyond the Larkin length scale [12,13] and thereby predict the existence of a new glassy state of anisotropic vortex matter, which because of its periodic positional order along columnar defects we refer to as “smectic” vortex glass. In Sec. IV we discuss the stability of the SmVG to dislocations and conclude in Sec. V with the summary, discussion, and open questions.

B. Summary of the results

As illustrated in Fig. 1(a), we focus on the large tilt angle, around a configuration of vortex lines transverse to columnar defects, staying away from the nontrivial vicinity of the critical field H_{\perp}^{c1} [33,37].

In this geometry, in the absence of point disorder, we predict that a qualitatively distinct, highly anisotropic “smectic” vortex glass [40] emerges. Structurally, it is characterized by a periodic vortex order *along* the translationally invariant columnar defects axis with smectic-like (but here δ -function

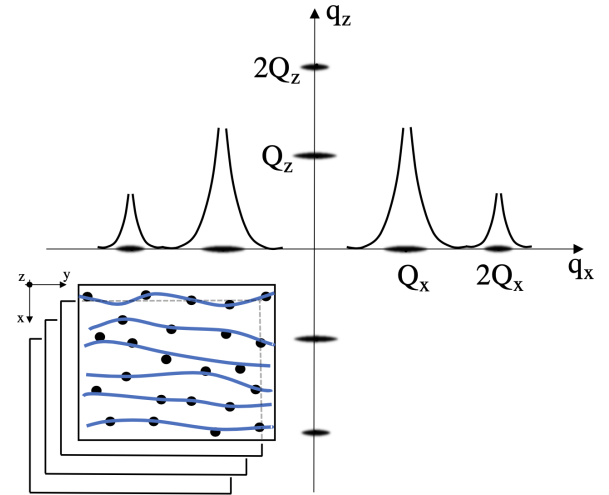


FIG. 2. A schematic form of the structure function $S(q_x, q_z)$ characterizing smectic vortex glass order. In the absence of point disorder it exhibits resolution-limited δ -function Bragg peaks along columnar defects (q_z) and universal quasi-Bragg peaks along the transverse axis (q_x).

“true”) Bragg peaks,

$$S(0, q_z) \sim \sum_n I_{nQ_z} \delta(q_z - nQ_z), \quad (1)$$

illustrated in Fig. 2, with $I_Q(T)$ a standard phonon Debye-Waller factor.

In contrast, vortices are randomly pinned transversely by cross sections of columnar defects (with each plane akin to a Cardy-Ostlund planar vortex glass [15–17]), with “rough” transverse distortions, which for weak disorder are logarithmically (rather than $\ln^2 L$) rough,

$$\frac{1}{2} \overline{\langle u(x) - u(0) \rangle^2} \approx Q_x^{-2} \eta \ln(x/a), \quad (2)$$

with the *universal* amplitude η computed to lowest order in $\epsilon = 5 - d$ expansion using functional renormalization group analysis, with $\eta \approx 2\pi^2/9$ in 3D (identical to that found in Ref. [19]). This asymptotic result is valid for lengths exceeding the Larkin scale,

$$\xi_L = a \sqrt{\tilde{K}^2 / \Delta}, \quad (3)$$

where \tilde{K} is the effective elastic constant and Δ the variance of the random force pinning disorder.

We thus predict that SmVG displays quasi-Bragg peaks [19], transverse to columnar defects,

$$S(q_x, 0) \sim \sum_n \frac{1}{|q_x - nQ_x|^{1-n^2\eta}}, \quad (4)$$

illustrated in Fig. 2, with a *universal* power-law exponent $\eta \approx 2\pi^2/9$. We note that if this approximate value of η is indeed greater than 1, we then predict only cusp singularities, rather than divergent quasi-Bragg peaks, to appear at the reciprocal lattice vectors, nQ_x , $n \in \mathbb{Z}$.

To the extent that the disorder imposed by columnar defects is perfectly correlated along their axis (taken as z), we predict that vortex planes of the SmVG, transverse to columnar defects, exhibit true 2D topological “Bragg” glass order

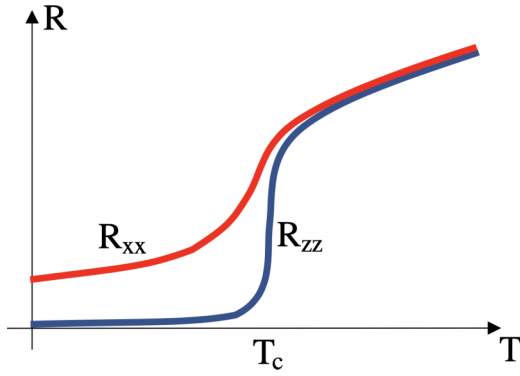


FIG. 3. A schematic illustration of infinitely anisotropic resistance (in the absence of additional point disorder) along R_{zz} and perpendicular R_{xx} to columnar defects characterizing the smectic vortex glass state. In a more realistic case of residual point pinning, at sufficiently low temperatures and long scales the state will freeze into a fully dissipationless superconducting highly anisotropic vortex glass.

[15,19,22,25,41,42], characterized by a vanishing dislocation density, with only elastic single-valued distortions as illustrated in Fig. 1(a) and the inset of Fig. 2.

For strong disorder and/or high temperature, dislocations may spontaneously proliferate, driving a topological transition to a fully disordered vortex-glass-like state [3], with transverse distortions characterized by a Lorentzian structure function along q_x .

Concomitantly, as illustrated in Fig. 3 we predict such smectic vortex glass state (in the idealized case of no additional pinning disorder) to exhibit a striking infinite resistive anisotropy. For current transverse to columnar defects and to the magnetic field, a free motion of vortices along homogeneous columnar defects leads to a nonzero flux-flow resistivity $\rho_{\perp} \sim (B/H_{c2})\rho_n$, with ρ_n resistivity arising from normal carriers residing in the vortex core, superfluid phase slip, and time-dependent flux associated with moving vortices. In contrast, for current along columnar defects vortex motion is impeded by columnar defects, exhibiting a vanishing linear resistivity of the vortex glass state [3,15]. Thus, we predict a vanishing of the resistivity ratio,

$$\rho_{zz}/\rho_{xx} \rightarrow 0, \quad (5)$$

inside the smectic vortex glass.

We also predict that the smectic vortex glass, viewed as an effective elastic medium, exhibits a vanishing response $\partial_z u_x$ to shear stress σ_{zx} in the zx plane transverse to applied magnetic field (i.e., transverse to vortex lines), defined by the columnar defects (z) axis. SmVG is thus characterized by a divergent shear modulus,

$$\mu_{zx} \rightarrow \infty. \quad (6)$$

However, unlike the Bose glass vortex state, where such divergent tilt modulus can be readily probed via a vanishing response to a magnetic field transverse to columnar defects—the “transverse Meissner effect” [28,32,33]—here there does not appear to be a simple way to probe the vanishing SmVG response corresponding to (6).

We now turn to the vortex model in this transverse geometry and to the derivation of these results.

II. MODEL OF THE SMECTIC VORTEX GLASS

In a type-II superconductor, for fields above a lower-critical field, H_{c1} , the magnetic flux penetrates in the form of interacting vortex flux lines carrying a unit of a fundamental flux quantum $\phi_0 = hc/2e$, with average density determined by the applied magnetic field [7]. At low temperature and in the absence of disorder, repulsive directed vortex lines crystallize into a periodic triangular array—an Abrikosov vortex lattice—whose elastic description [1,43,44] can be derived from the Ginzburg-Landau theory for the superconducting order parameter, which itself, under certain conditions, is derivable from the microscopic theory.

A. Elasticity and columnar pinning for a transverse magnetic field

Transcending such a detailed derivation, on sufficiently long length scale the elastic vortex lattice energy functional can be deduced purely on symmetry grounds. In three-dimensions, it is formulated in terms of a two-dimensional Eulerian phonon vector field (Goldstone modes of the spontaneously broken translational symmetry) $\mathbf{u}(\mathbf{r}_{\perp}, y) = (u_x(x, y, z), u_z(x, y, z))$ describing vortex lattice distortion in the x - z plane [spanned by $\mathbf{r}_{\perp} = (x, 0, z)$], transverse to the vortex lines, which we take to run along the y axis, as illustrated in Fig. 1(a).

Such a triangular vortex crystal state is then characterized by an elastic energy that, in the absence of other ingredients, is an isotropic functional of \mathbf{u} ,

$$H_{\text{el}} = \int_{\mathbf{r}} \left[\frac{K}{2} (\partial_y \mathbf{u})^2 + \mu u_{ij}^2 + \frac{\lambda}{2} u_{ii}^2 \right], \quad (7)$$

with $\int_{\mathbf{r}} \equiv \int d^2 r_{\perp} dy \equiv \int dx dz$, $\mathbf{x} = (x, y, 0)$, K a tilt modulus, and μ, λ the elastic Lamé coefficients [46].

A random array of parallel columnar defects (see Fig. 1) oriented along $\hat{\mathbf{z}}$ transversely to vortex lines along $\hat{\mathbf{y}}$ introduces a random highly anisotropic pinning potential $V(x, y)$ that couples to the two-dimensional [in a plane spanned by $\mathbf{r}_{\perp} = (x, 0, z)$] vortex density,

$$n(\mathbf{r}) \approx n_0 - n_0 \nabla_{\perp} \cdot \mathbf{u} + \sum_{\mathbf{Q}} n_{\mathbf{Q}} e^{i\mathbf{Q} \cdot [\mathbf{r}_{\perp} + \mathbf{u}(\mathbf{r})]}, \quad (8)$$

and a random tilting potential $\delta K_i(x, y)$, which for the $\pi/2$ transverse-field geometry of Fig. 1(a) couples to the even power of the vortex lattice tilt $\partial_y \mathbf{u}$, thereby preserving the $\pm \partial_y \mathbf{u}$ symmetry. The resulting pinning energy functional is given by [45]

$$H_{\text{pin}} = \int_{\mathbf{r}} \left[\frac{\delta K_i(x, y)}{2} (\partial_y u_i)^2 + n_0 V(x, y) \nabla_{\perp} \cdot \mathbf{u} - V(x, y) \sum_{\mathbf{Q}} n_{\mathbf{Q}} e^{i\mathbf{Q} \cdot [\mathbf{r}_{\perp} + \mathbf{u}(\mathbf{r})]} \right], \quad (9)$$

where n_0 is the average density and $n_{\mathbf{Q}}$ are the Fourier components of the vortex density at the discrete set of reciprocal lattice vectors, \mathbf{Q} . By symmetry, the average columnar defect

density results in a biaxial lattice anisotropy [46] and the tilt modulus, with correction $\delta K_i = \delta \bar{K}_i(x, y)$, expected to be $\delta K_z < 0$ and $\delta K_x \approx 0$. This can be accounted for by $K \rightarrow K_i$. Because $\delta K_i(x, y)$ is coupled to the square of the vortex tilt, for weak heterogeneity fluctuations around its average are subdominant at long scales.

Furthermore, because columnar defects are translationally invariant, the corresponding pinning potential $V(x, y)$ is z independent, and thus long-wavelength pinning $\int_{\mathbf{r}} n_0 V(x, y) \nabla_{\perp} \cdot \mathbf{u}$ reduces to $\int_{\mathbf{r}} U_0(x, y) \partial_x u_x$, only coupling to the $u_x(x, y)$ displacement transverse to the columnar defect. As in other random pinning problems [19,41,42] standard analysis shows that the long-wavelength part of the pinning is perturbatively subdominant for weak disorder in 3D (in contrast to the 2D Fisher-Cardy-Ostlund pinning, where it leads to a super-rough glass [15–17] with $\ln^2 r$ correlations). However, as we will see it does play a role at asymptotic scales in the physical 3D case.

The z independence of $V(x, y)$ also reflects itself in the averaging out of the short-scale density components $n_{\mathbf{Q}}$ with a nonzero $Q_z \hat{\mathbf{z}}$ reciprocal lattice vector. Thus, $u_z(\mathbf{r})$ only appears harmonically, and the nonlinear short-scale pinning only acts on $u_x(\mathbf{r})$. The full effective Hamiltonian then reduces to [45]

$$H = \int_{\mathbf{r}} \left[\frac{1}{2} u_i \hat{\Gamma}_{ij} u_j + U_0(x, y) \partial_x u_x + U(x, y, u_x(\mathbf{r})) \right], \quad (10)$$

where we take $U_0(x, y)$ to be characterized by a zero-mean Gaussian distribution with variance R_0 ,

$$\overline{U_0(x, y) U_0(x', y')} = R_0 \delta(x - x') \delta(y - y'). \quad (11)$$

The short-scale pinning potential,

$$U(x, y, u_x(\mathbf{r})) = \sum_{\mathbf{Q}} U_{\mathbf{Q}}(x, y) e^{i\mathbf{Q}u_x(\mathbf{r})}, \quad (12)$$

has Fourier component at $\mathbf{Q} \equiv \mathbf{Q}_x$ given by

$$U_{\mathbf{Q}}(x, y) = - \int_{\text{unit-cell at } x} \delta \delta x V(x + \delta x, y) n_{\mathbf{Q}} e^{i\mathbf{Q}\delta x}, \quad (13)$$

and we take it to be zero mean, Gaussian correlated, and characterized by a variance

$$\overline{U(x, y, u_x) U(x', y', u'_x)} = R(u_x - u'_x) \delta(x - x') \delta(y - y'). \quad (14)$$

The periodicity of $U(x, y, u_x + 2\pi/\mathbf{Q}) = U(x, y, u_x)$ [and therefore of $R(u_x)$] in u_x reflects the identity symmetry of vortex lines. The Fourier transform of the inverse propagator $\hat{\Gamma}_{ij}$ (for now ignoring (here) unimportant anisotropies [46]) is given by

$$\Gamma_{ij}(\mathbf{q}) = (Kq_y^2 + \mu q_{\perp}^2) P_{ij}^T + [Kq_y^2 + (2\mu + \lambda)q_{\perp}^2] P_{ij}^L, \quad (15)$$

with $P_{ij}^{T,L}(\mathbf{q}_{\perp})$ the transverse and longitudinal projection operators with respect to \mathbf{q}_{\perp} .

B. Reduction to a correlated random-field xy model

It is now quite clear how to proceed. Because u_z only enters the Hamiltonian harmonically, we can integrate it out exactly, obtaining an effective xy model for a single phonon u_x that is nontrivially pinned by a z -independent random potential, that

is short-ranged in the x - y plane. Standard analysis gives an effective Hamiltonian

$$\tilde{H} = \int_{\mathbf{r}} \left[\frac{1}{2} u_x \hat{\Gamma} u_x + U_0(x, y) \partial_x u_x + U(x, y, u_x(\mathbf{r})) \right], \quad (16)$$

where $\hat{\Gamma}$ is the effective elastic kernel, whose Fourier transform $\tilde{\Gamma}(\mathbf{q}) = (\Gamma_{xx}\Gamma_{zz} - \Gamma_{xz}^2)/\Gamma_{zz} = 1/(\hat{\Gamma}^{-1})_{xx}$ is given by

$$\tilde{\Gamma}(q_x, q_y, q_z) = \frac{(Kq_y^2 + \mu q_{\perp}^2)[Kq_y^2 + (2\mu + \lambda)q_{\perp}^2]}{[Kq_y^2 + \mu q_{\perp}^2 + (\mu + \lambda)q_z^2]}. \quad (17)$$

As expected, though long-ranged, it scales as q^2 , by power-counting akin to a random field xy model.

Minimization of H in (10) over u_z shows that in the ground state (relevant for zero temperature), neglecting boundary contributions and possible random symmetry breaking along z (possible for strong disorder),

$$\hat{\Gamma}_{zz} u_z = -(\mu + \lambda) \partial_z \partial_x u_x(x, y) = 0. \quad (18)$$

Thus, as anticipated, vortex lattice phonons along columnar defects, u_z , experience no disorder-induced distortions or pinning [45], fully controlled by thermally induced fluctuations. The corresponding two-point correlator $C_{zz}(\mathbf{r}) = \frac{1}{2} \overline{[u_z(\mathbf{r}) - u_z(0)]^2}$ is then given by

$$C_{zz}(\mathbf{r}) = T \int_{\mathbf{q}} \frac{[Kq_y^2 + \mu q_{\perp}^2 + (\mu + \lambda)q_x^2](1 - e^{i\mathbf{q}\cdot\mathbf{r}})}{(Kq_y^2 + \mu q_{\perp}^2)[Kq_y^2 + (2\mu + \lambda)q_{\perp}^2]}, \quad (19)$$

$$\mathbf{r} \rightarrow \infty = u_{z,\text{rms}}^2 \approx \frac{T}{Ka},$$

where \bar{K} is an effective stiffness (a function of K, μ, λ) whose detailed form is unimportant, and $a \sim 2\pi/\Lambda$ is lattice cutoff. As indicated above, the key point is that in 3D this integral is convergent at small wave vectors and thus at long scales the phonon correlator asymptotes to a finite \mathbf{r} -independent constant, and therefore at low temperature exhibits a stable periodic (layered) smectic order along columnar defects. We thus expect at low T the structure function for vortex configuration transverse to columnar defects, Fig. 1(a), to exhibit true smectic Bragg peaks for momentum transfer along columnar defects (q_z), with amplitude reduced by a Debye-Waller factor, $e^{-Q_z^2 u_{z,\text{rms}}^2}$, as illustrated in Fig. 2.

As the temperature is raised, at sufficiently high T , such that $u_{z,\text{rms}}$ increases to a fraction of a lattice constant—a Lindemann criterion—we expect that the smectic order will melt at a temperature

$$T_{\text{melt-Sm}} \approx c_L a^3 \bar{K}, \quad (20)$$

where c_L is a Lindemann number of order 0.1–0.2, to be fitted by experiments. At low temperature below $T_{\text{melt-Sm}}$, the SmVG state is stable and the nontrivial part of the problem reduces to a pinning-induced distortion of a single phonon, u_x , transverse to columnar defects.

III. PINNING OF TRANSVERSE PHONONS

We now study Hamiltonian (16), analyzing the statistics of the transverse phonon $u_x(x, y)$ in the presence of Gaussian short-range correlated z -independent pinning potentials, $U(\mathbf{x}, u_x(\mathbf{x}, z)), U_0(\mathbf{x})$, and elastic kernel $\tilde{\Gamma}(\mathbf{q})$, (17).

A. Perturbative Larkin analysis

Vortex lattice $u_x(\mathbf{r})$ distortions are characterized by a sum of thermal and random pinning contributions, $C_{xx}(\mathbf{r}) = C_{xx}^T(\mathbf{r}) + C_{xx}^\Delta(\mathbf{r})$, where

$$C_{xx}^T(\mathbf{r}) = \frac{1}{2} \overline{[u_x(\mathbf{r}) - u_x(0)]^2}_c, \quad (21)$$

$$C_{xx}^\Delta(\mathbf{x}) = \frac{1}{2} \overline{[u_x(\mathbf{r}) - u_x(0)]^2}, \quad (22)$$

where subscript c denotes ‘‘connected’’ correlation function $\langle \phi \phi \rangle_c \equiv \langle (\phi - \langle \phi \rangle)^2 \rangle = \langle \phi \phi \rangle - \langle \phi \rangle \langle \phi \rangle$. Above, in contrast to the thermal component, $C_{xx}^T(\mathbf{r})$, we explicitly indicated $C_{xx}^\Delta(\mathbf{x})$ to be a function of \mathbf{x} , rather than full $\mathbf{r} = (\mathbf{x}, z)$, i.e., independent of z . At short scales, such that u_x phonon distortions are small compared to the lattice constant and disorder correlation length, we can follow Larkin [12] and expand the random potential $U(\mathbf{x}, u_x(\mathbf{x}))$ in H , (10) or (16), to linear order in $u_x(\mathbf{x})$ about an undistorted state (a random force approximation equivalent to the Imry-Ma estimate), which can be then analyzed exactly in this perturbative regime [12,13,19,41,42].

At low temperature $C_{xx}^\Delta(\mathbf{x}) \equiv G_{xx}^\Delta(0) - G_{xx}^\Delta(\mathbf{x})$ dominates, with phonon correlations captured by the propagator $G_{xx}^\Delta(\mathbf{x}) = \overline{u_x(\mathbf{r}) \langle u_x(0) \rangle}$, and mean-squared distortions given by

$$G_{xx}^\Delta(0) \approx \int_{\mathbf{q}_x, q_y} \frac{\Delta}{|\tilde{\Gamma}(\mathbf{q}_x, q_y, 0)|^2} \quad (23)$$

$$\approx \int_{\mathbf{q}_x, q_y} \frac{\Delta}{[Kq_y^2 + (2\mu + \lambda)\mathbf{q}_x^2]^2}$$

$$= \frac{\Delta}{\pi \tilde{K}^2} L^2, \quad \text{for } d = 3, \quad (24)$$

$$= \frac{C_{d-2} \Delta}{\tilde{K}^2} L^{5-d}, \quad \text{for } d < 5, \quad (25)$$

where $\tilde{K}^2 \equiv \sqrt{K(2\mu + \lambda)^3}$ is the effective elastic constant, $\Delta \equiv \Delta(0) = -R'(0)$ is the random force correlator, and in the last equality, for later convenience, we generalized the analysis to d dimensions, denoting d -dimensional coordinate vector $\mathbf{r} \equiv (\mathbf{x}, z)$ and $(d-1)$ -dimensional coordinate vector transverse to $\hat{\mathbf{z}}$ as $\mathbf{x} = (\mathbf{x}_\perp, y)$. Above, for convenience we chose a cylindrical momentum cutoff with $-\infty < q_y < \infty$ and defined $C_d = S_d / (2\pi)^d = 2\pi^{d/2} / \Gamma(d/2) / (2\pi)^d$ [$C_1 = 1/\pi$, $C_3 = 1/(2\pi^2)$], with S_d a surface area of a d -dimensional unit sphere. In the above analysis we also neglected the long-wavelength disorder $U_0(\mathbf{x})$, which is subdominant at scales shorter than ξ_L , where it gives distortions that scale logarithmically in $d = 3$, and are finite for $d > 3$.

The above strongly divergent u_{rms} distortions are expected due to the correlated z -independent random columnar potential, contrasting with the corresponding point-disorder L^{4-d} growth [12,13,19,41,42]. For $d < d_c = 5$ the perturbative result (25) predicts its own breakdown at sufficiently long scales $L > \xi_L$, where the Larkin correlation length [up to constants of $O(1)$] is given by

$$\xi_L = (a^2 \tilde{K}^2 / \Delta)^{1/(5-d)}. \quad (26)$$

Through this perturbative analysis, a combination of (19) and (25) predicts that in the physical case of three dimensions, vortex configurations transverse to columnar defects

[Fig. 1(a)] are characterized by a periodic order along columnar defects, with $u_{\text{rms}}^z \ll a$ at low T and divergent distortions, u_{rms}^x perpendicular to columnar defects, which we will show grow logarithmically on scales longer than ξ_L . Thus, as illustrated in Figs. 1(a), 1(b) and 2, this 3D transverse vortex state, which we dubbed a ‘‘smectic vortex glass,’’ is an array of y -directed vortex sheets confined to the x - y plane, exhibiting long-range periodic order along the $\hat{\mathbf{z}}$ -directed columnar defects, with true Bragg peaks along q_z (2), and, as we will show below, quasi-long-range order (characterized by quasi-Bragg peaks) within the x - y plane.

B. Replicated model

We now focus on the positional order within the \mathbf{x}_\perp - y plane transverse to columnar defects, characterized by distortions $u(\mathbf{r}) \equiv u_x(\mathbf{r})$, where for simplicity of notation we have dropped subscript x .

To compute self-averaging quantities (e.g., the disorder-averaged free energy and correlation functions) it is convenient (but not necessary) to employ the replica ‘‘trick’’ [18], which allows us to work with a translationally invariant field theory at the expense of introducing n replica fields, with the $n \rightarrow 0$ limit to be taken at the end of the calculation. For the free energy this procedure relies on the identity for the $\ln z$ function

$$\overline{\ln z} = -T \overline{\ln Z} = -T \lim_{n \rightarrow 0} \frac{\overline{Z^n} - 1}{n}. \quad (27)$$

After replicating and integrating over the random potential $U[u(\mathbf{r}), \mathbf{x}]$ using (14), we obtain

$$\overline{Z^n} = \int [du_\alpha] e^{-H^{(r)}[u_\alpha(\mathbf{r})]/T}. \quad (28)$$

The effective translationally invariant replicated Hamiltonian $H^{(r)}[u_\alpha(\mathbf{r})]$ is given by

$$H^{(r)} = \frac{1}{2} \sum_{\alpha}^n \int_{\mathbf{x}, z} [u_\alpha \hat{\Gamma} u_\alpha + \mu_{zx} (\partial_z u_\alpha)^2]$$

$$- \frac{1}{2T} \sum_{\alpha, \beta}^n \int_{\mathbf{x}, z, z'} R[u_\alpha(\mathbf{x}, z) - u_\beta(\mathbf{x}, z')], \quad (29)$$

where we added an additional elastic term, characterized by a shear modulus μ_{zx} , which we expect to be generated under coarse-graining. We will use this Hamiltonian (29) in our subsequent renormalization group analysis of the system.

C. Physics beyond Larkin scale: Functional renormalization group

As we saw in the Larkin analysis of Sec. III A, at scales shorter than ξ_L , the transverse phonon distortions u are small compared to the lattice constant and disorder correlation length, and thus have been treated perturbatively [12,13,19,41,42]. The growth of $u_{\text{rms}} \sim L^{(5-d)/2}$ in (25) is indicative of highly nonlinear, nonperturbative effects of disorder at scales beyond ξ_L , requiring a functional renormalization group (FRG) treatment [41], which can be controlled in an expansion in $\epsilon = 5 - d$ about the lower-critical dimension, $d_{lc} = 5$.

To this end it is convenient to work with the translationally invariant replicated Hamiltonian, $H^{(r)}$, (29). We employ the standard momentum-shell RG transformation [41,47], by separating the phonon field into a long and short scale contributions according to $u_\alpha(\mathbf{r}) = u_\alpha^<(\mathbf{r}) + u_\alpha^>(\mathbf{r})$ and perturbatively in nonlinearity $R[u_\alpha^>(\mathbf{x}, z) - u_\beta^>(\mathbf{x}, z')]$ integrate out the high-wave-vector components $u_\alpha^>(\mathbf{r})$, which take support in an infinitesimal shell $\Lambda/b < q < \Lambda \equiv 1/a$, with $b = e^{\delta\ell}$. We follow this with a rescaling of lengths and the long-wavelength part of the field,

$$\mathbf{x} = b\mathbf{x}', \quad (30)$$

$$z = b^\omega z', \quad (31)$$

$$u^<(b\mathbf{x}', b^\omega z') = u'(\mathbf{x}', z), \quad (32)$$

so as to restore the UV cutoff back to Λ . Based on disorder correlated along z we anticipated a nontrivial anisotropy between \mathbf{x} and z , encoded in $\omega \approx 1 + O(\epsilon)$. In Eq. (32) we made a convenient choice of a zero scaling dimension for the real-space displacement field $u(\mathbf{x}, z)$. This is dictated by the convenience of keeping the periodicity of the disorder variance $R(u)$ fixed at $2\pi/Q$.

The above rescaling leads to zeroth-order RG flows of the effective elastic constant \tilde{K} (which represents K, μ, λ), μ_{zx} , and disorder pinning potential $R(u)$, which are given by

$$\tilde{K}(b) = b^{d-3+\omega}\tilde{K}, \quad (33)$$

$$\mu_{zx}(b) = b^{d-1-\omega}\mu_{zx}, \quad (34)$$

$$R(u, b) = b^{d-1+2\omega}R(u), \quad (35)$$

indicating that in $d > 2$ the effective strengths of both elastic and pinning energies grow at long scales relative to the thermal energy, T . This is a reflection that in $d > 2$ the physics is controlled by the zero-temperature ground-state competition between elastic and pinning energies, at long scales both much larger than the thermal energy. Equivalently, to emphasize this physics we can rescale T according to

$$T(b) = b^{-(d-3+\omega)}T \quad (36)$$

$$\equiv b^{-\Theta}T, \quad (37)$$

with $\Theta \approx d - 2 + O(\epsilon)$, so as to keep the elastic energy fixed at order 1. With this convenient rescaling convention, the measure of the effective pinning strength grows according to

$$R(u, b) = b^{5-d}R(u), \quad (38)$$

modified by a factor $[T(b)/T]^2 = b^{-2\Theta}$ relative to that in Eq. (35) due to the factor of $1/T^2$ in $H^{(r)}/T$, (29). Equivalently, without the rescaling of T , the dimensionless combination that arises in the coarse-graining analysis is given by $R(u)/\tilde{K}^2$, and its zeroth-order flow is given by Eq. (38).

In either convention we find that for $d < d_{lc} = 5$, the Gaussian disorder-free fixed point is unstable, indicating that the influence of random pinning grows at long scales relative to the elastic energy, consistent with the scaling and Larkin analysis above.

The statistical symmetry [17,19,41,42] of the bulk Hamiltonian H , (10), under an arbitrary local distortion, $u(\mathbf{x}, z) \rightarrow u(\mathbf{x}, z) + \chi(\mathbf{x})$, guarantees that the flow of $\tilde{K}(b)$, (33), and, equivalently, the thermal exponent,

$$\Theta = d - 3 + \omega \approx d - 2 + O(\epsilon), \quad (39)$$

are *exact*, i.e., do not experience any coarse-graining corrections. This can equivalently be seen from the replicated Hamiltonian (29), where the pinning nonlinearity, $R[u_\alpha(\mathbf{x}, z) - u_\beta(\mathbf{x}, z')]$, depends only on the difference between fields at distinct z coordinates and replicas, i.e., independently of the ‘‘center of mass’’ field $\sum_{\alpha=1}^n u_\alpha(\mathbf{x})$. That is, the only nonlinearity in $H^{(r)}$ exhibits a symmetry of a replica- and z -independent local distortion $u_\alpha(\mathbf{x}, z) \rightarrow u_\alpha(\mathbf{x}, z) + \chi(\mathbf{x})$ and under coarse-graining can therefore only generate terms that also exhibit this symmetry. Thus, it cannot generate a correction to the elastic term that clearly lacks this symmetry, implying that \tilde{K} is *not* renormalized by the pinning disorder. In contrast, as we discuss below, the shear modulus μ_{zx} indeed is strongly renormalized by the pinning potential under coarse-graining.

1. Pinning

An important consequence of the periodic nonlinearity $R(u)$ and the effective zero-temperature physics, first emphasized by Fisher [41], is that all monomials or (equivalently) harmonics in the expansion of $R(u)$ are equally relevant in $2 - O(\epsilon) < d < d_{lc} = 5$. Thus, a *functional* RG analysis that follows the coarse-graining flow of the whole *function* $R(u, b)$ is necessary. The method is by now quite standard [19,41,42] and is straightforwardly adapted to the correlated pinning problem [32], characterized by $H^{(r)}$, Eq. (29).

We limit the FRG analysis to one-loop order, performing the momentum-shell integration over the high-wave-vector components $u_\alpha^>$ perturbatively in the nonlinearity $H_p = -\frac{1}{2T} \sum_{\alpha,\beta} \int_{\mathbf{x},z,z'} R[u_\alpha(\mathbf{x}, z) - u_\beta(\mathbf{x}, z')]$, and controlled by an $\epsilon = 5 - d$ expansion. The correction to the Hamiltonian due to the coarse-graining is given by

$$\delta H^{(r)}[u_\alpha^<] = \langle H_p[u_\alpha^< + u_\alpha^>] \rangle - \frac{1}{2T} \langle H_p^2[u_\alpha^< + u_\alpha^>] \rangle^c \dots, \quad (40)$$

where the averages over short-scale fields $u_\alpha^>$ above are performed with the quadratic (elastic \tilde{K}) part of $H^{(r)}$. The superscript c denotes a cumulant average, $\langle H_p^2 \rangle^c = \langle H_p^2 \rangle - \langle H_p \rangle^2$.

Based on Eqs. (37) and (39), temperature is (dangerously) irrelevant for $d > 2$, and we thus focus on the zero-temperature limit, in which the lowest-order contribution

comes at a second order in $R(u)$, given by

$$\delta H^{(r)} \approx -\frac{1}{16T^3} \sum_{\alpha_1, \beta_1, \alpha_2, \beta_2} \int_{\mathbf{x}_1, z_1, z'_1}^{\mathbf{x}_2, z_2, z'_2} R''[u_{\alpha_1}^<(\mathbf{x}_1, z_1) - u_{\beta_1}^<(\mathbf{x}_1, z'_1)] R''[u_{\alpha_2}^<(\mathbf{x}_2, z_2) - u_{\beta_2}^<(\mathbf{x}_2, z'_2)] I_{\alpha_1 \beta_1}^{\alpha_2 \beta_2}(\mathbf{x}_1, z_1, z'_1; \mathbf{x}_2, z_2, z'_2), \quad (41)$$

where in the above, the prime indicates a partial derivative with respect to u , and

$$\begin{aligned} I_{\alpha_1 \beta_1}^{\alpha_2 \beta_2} &= \frac{1}{2} [(u_{\alpha_1}^>(\mathbf{x}_1, z_1) - u_{\beta_1}^>(\mathbf{x}_1, z'_1)) \text{big}]^2 [u_{\alpha_2}^>(\mathbf{x}_2, z_2) - u_{\beta_2}^>(\mathbf{x}_2, z'_2)]^2 \\ &= 8 \left[\frac{1}{2} \delta_{\alpha_1 \alpha_2} \delta_{\beta_1 \beta_2} G_T^>(\mathbf{x}_1 - \mathbf{x}_2, z_1 - z_2) G_T^>(\mathbf{x}_1 - \mathbf{x}_2, z'_1 - z'_2) - \delta_{\alpha_1 \alpha_2} \delta_{\beta_1 \beta_2} G_T^>(\mathbf{x}_1 - \mathbf{x}_2, z_1 - z_2) G_T^>(\mathbf{x}_1 - \mathbf{x}_2, z_1 - z'_2) \right]^2. \end{aligned} \quad (42)$$

Above we kept only the most relevant two-replica thermal terms, with a thermal (zero-disorder) momentum-shell propagator, $G_T^>(\mathbf{x}, z) = \langle u^>(\mathbf{x}, z) u^>(0, 0) \rangle_0^>$. Using the short-range property of this propagator and comparing to H_p , we then obtain

$$\delta R(u) \approx \delta \ell g_2 \left(\frac{1}{2} R''(u) R''(u) - R''(u) R''(0) \right), \quad (43)$$

where the constant g_2 is defined by

$$\begin{aligned} g_2 \delta \ell &= T^{-2} \int_{\delta \mathbf{x}, \delta z, \delta z'} G_T^>(\delta \mathbf{x}, \delta z) G_T^>(\delta \mathbf{x}, \delta z') \\ &= \int_{\mathbf{q}_x, q_y}^> \frac{1}{|\tilde{\Gamma}(\mathbf{q}_x, q_y, 0)|^2} \\ &= \int_{\Lambda e^{-\delta \ell}}^{\Lambda} \frac{d^{d-2} q_x}{(2\pi)^{d-2}} \int_{-\infty}^{\infty} \frac{dq_y}{2\pi} \frac{1}{[K q_y^2 + (2\mu + \lambda) \mathbf{q}_x^2]^2} \\ &= \frac{C_{d-2} \Lambda^{d-5}}{\sqrt{K(2\mu + \lambda)^3}} \delta \ell. \end{aligned} \quad (44)$$

Combining this with the rescalings Eq. (33)–(35), we obtain the FRG flow equation for a dimensionless measure of pinning disorder, $\hat{R}(u) \equiv g_2 R(u)$,

$$\partial_\ell \hat{R}(u) = \epsilon \hat{R}(u) + \frac{1}{2} \hat{R}'(u) \hat{R}''(u) - \hat{R}''(u) \hat{R}''(0). \quad (45)$$

We note that aside from constant prefactors (g_2) in the definition of $\hat{R}(u, \ell)$ and the raised (from 4 to 5) lower-critical dimension giving $\epsilon = 5 - d$, this FRG flow is identical to that of the uncorrelated pinning disorder [19,41,42], with the fixed point function for the random force correlator given by

$$\hat{\Delta}_*(u) = -\hat{R}''_*(u) = \frac{\epsilon}{6Q^2} \left[(Qu - \pi)^2 - \frac{\pi^2}{3} \right], \quad (46)$$

periodically extended with period $2\pi/Q$.

2. Breakdown of elasticity

As noted above, elastic moduli K, μ, λ characterizing z -independent distortions $u(\mathbf{x}, y)$ are protected by the \mathbf{x} - y plane statistical symmetry, and thus remain fixed under coarse-graining. In contrast, it is straightforward to show that the μ_{zx} modulus for $\partial_z u$ shear is strongly enhanced by pinning, acquiring a correction

$$\delta \mu_{zx} \approx -g_2 \Delta''(0) \mu_{zx} \delta \ell, \quad (47)$$

that in the absence of point disorder and at zero temperature is divergent since $\Delta(u)$, (46), exhibits slope discontinuity at $u = 0$.

To understand the physical implications of this result requires a careful analysis of the dangerously irrelevant temperature and/or point disorder, neglected so far. These smoothen the $u = 0$ singularity within the boundary layer that shrinks on coarse-graining with ℓ . Conveniently, such analysis has been carefully done in Ref. [32] for a physically distinct but mathematically related “toy” model of a Bose glass. The upshot is that pinning generates a nonanalytic term,

$$\delta H = \frac{1}{2} \sigma_c \int_{\mathbf{x}} |\partial_z u|, \quad (48)$$

arising from the singularity $\Delta(u) \sim -|u| + \text{constant}$ around $u = 0$ outside the boundary layer. As discussed in Ref. [32], this results in a finite threshold σ_c response to an external shear stress σ_{zx} , with coupling $\sigma_{zx} \partial_z u$. This is the SmVG’s counterpart of the “transverse Meissner effect” in the Bose glass geometry (with field oriented along columnar defects) [28]. However, in contrast, here it is unclear to us how to probe this novel, effectively divergent μ_{zx} , characteristic of the SmVG.

3. Correlation function

With this RG analysis in hand, we can now calculate the transverse correlation function $C_{xx}^\Delta(\mathbf{x})$, (22), that dominates the asymptotics of vortex line distortions at scales beyond the perturbative Larkin scale. To this end we first examine the corresponding momentum correlation function,

$$C(\mathbf{q}) \equiv \frac{\overline{u(\mathbf{q})} \overline{u(\mathbf{q}')}}{\delta^d(\mathbf{q} + \mathbf{q}') \delta(q_z)}. \quad (49)$$

To compute this function we utilize the standard RG matching analysis [19,42], that allows us to relate a correlation function at a small wave vector \mathbf{q}_x of our interest (which is impossible to calculate in perturbation theory due to the infrared divergences) to the same correlation function at a large wave vector, $b\mathbf{q}_x$, which can be straightforwardly calculated in a controlled perturbation theory,

$$C(\mathbf{q}_x, q_y, 0) = b^{d-1} C(b\mathbf{q}_x, bq_y, 0, K, \mu, \lambda, R(u, b)). \quad (50)$$

Choosing $b\mathbf{q}_x = \Lambda$ for small \mathbf{q}_x , such that b is large to take $R(u, b \gg 1) \rightarrow R_*(u)$ to its fixed point (46), and computing

the right-hand side perturbatively in disorder, we find

$$C(\mathbf{q}_x, q_y, 0) = \frac{1}{q_x^{d-1}} \frac{\hat{\Delta}_*(0)\Lambda^{d-5}/g_2}{[K(q_y/q_x)^2 + (2\mu + \lambda)]^2}. \quad (51)$$

In coordinate space, at long scales beyond ξ_L , we find (for equal y separation)

$$C(\mathbf{x}) = \frac{1}{2} \overline{(u(\mathbf{x}) - u(0))^2} \approx Q^{-2} \eta_d \ln(x/a), \quad (52)$$

for all dimensions d in the range $2 - O(\epsilon) < d < 5$, where A is a universal amplitude that to one-loop order is given

$$\eta_d = \frac{\pi^2 \epsilon}{9}, \quad (53)$$

identical to that found in Refs. [19,32].

These translational correlations are best probed by the structure function, a Fourier transform of the density-density correlation function,

$$S(\mathbf{q}) = \sum_{\mathbf{r}_n^\perp} e^{-i\mathbf{q} \cdot \mathbf{r}_n^\perp} \overline{\langle e^{i\mathbf{q} \cdot [\mathbf{u}(\mathbf{r}_n^\perp) - \mathbf{u}(0)]} \rangle}. \quad (54)$$

For scattering along columnar defects, $\mathbf{q} = q_z \hat{\mathbf{z}}$, and using finite u_z distortions set by $u_{z,\text{rms}}$, Eq. (19), we find “true” δ -function Bragg peaks, suppressed by the thermal Debye-Waller factor, $I_{Q_z} = e^{-Q_z^2 T / (\bar{K}a)}$, as advertised in Eq. (1).

In contrast, for scattering at a wave vector $\mathbf{q} = q_x \hat{\mathbf{x}}$, transverse to columnar defects and the applied field (vortex lines), we utilize the Gaussian approximation (which amounts to ignoring higher-order cumulants) and the u_x - u_x correlation function computed above, (52). We thereby find

$$\begin{aligned} S(q_x) &= \sum_{x_n} e^{-iq_x x_n} e^{-q_x^2 C(x_n)} \\ &\approx \sum_{x_n} e^{-iq_x x_n} \frac{1}{|x_n|^{\eta_{ax}}} \\ &\sim \sum_p \frac{1}{|q_x - pQ_x|^{1-p^2\eta}}, \end{aligned} \quad (55)$$

where the universal power-law exponent in 3D $\eta = \eta_3 \approx 2\pi^2/9$, and we utilized the Poisson summation formula to perform x_n summation. We note that if this approximate value of η is indeed greater than 1, only cusp singularities, rather than divergent quasi-Bragg peaks, will appear at the reciprocal lattice vectors, Q_x .

IV. DISLOCATIONS

As with other pinning problems [19–22,41,42], the above analysis notwithstanding, a vexing problem is that of topological defects. Namely, it is important to assess the stability of the SmVG phase to a proliferation of dislocations. For strong disorder, at high temperatures, and/or in the presence of point disorder, these will undoubtedly proliferate, destroying the topologically ordered (Bragg glass) character of the SmVG. However, at weak disorder and low temperatures, one can contemplate that dislocation-free Bragg glass order [19,22,42] will persist to arbitrary scales of the SmVG state. Otherwise, our above results will extend only out to a dislocation scale, ξ_D (set by the average spacing of proliferated dislocations),

that will be long in the limit of weak disorder and low temperatures, thereby allowing a broad range of SmVG regime.

In addition to these generic considerations [19,22,42], which are extremely challenging to rigorously assess, we believe considerations of SmVG are much more favorable for its stability against dislocations. It is made so by the translational invariance of disorder along columnar defects (z axis) and vortices running transverse to them. This is based on the fact that for SmVG, (i) Eq. (18) strictly gives $u_z = 0$ in the ground state, (ii) it gives convergent thermal $u_{z,\text{rms}}$ fluctuations, that can be made arbitrarily small at low T according to (19), and (iii) all observables are expected to be z independent in the ground state (neglecting the possibility of spontaneous inhomogeneous symmetry breaking along columnar defects at strong disorder).

To examine these arguments in more detail, we note that a potential dislocation density in SmVG is defined by a non-single-valued displacement field,

$$\hat{\mathbf{y}} \cdot \nabla \times \nabla u_i = b_i(\mathbf{r}). \quad (56)$$

A key consequence of property (iii), the z independence of vortex distortions, $u_i(\mathbf{x})$, is that gradients in (56), acting within the x - z plane, immediately imply a vanishing of dislocation density, $b_i(\mathbf{r}) = 0$.

In addition, we can focus on vortex line order within the x - y planes, with vortices running along the y axis, as illustrated in Fig. 1(a). Based on properties (i) and (ii), at low temperature and weak disorder, we can neglect vortex distortions along columnar defects, taking $u_z = 0$. We then note that with these conditions, within the x - y planes, the system reduces to an array of “1 + 1”-dimensional systems of Fisher’s vortex glass [15]. Based on this, it is obvious that magnetic flux conservation (vortex line continuity) immediately forbids dislocations (partial lines) within these x - y vortex planes. This can be seen mathematically by observing that components of the magnetic flux are generically given by $\mathbf{B} = B_0(\partial_y u_x, -\nabla \cdot \mathbf{u}, \partial_y u_z)$, and for $u_z \approx 0$ reduce to

$$B_x = B_0 \partial_y u_x, \quad B_y = -B_0 \partial_x u_x. \quad (57)$$

Thus, the vanishing divergence of flux density (absence of monopoles), $\nabla \cdot \mathbf{B} = 0$, reduces to

$$\partial_x \partial_y u_x - \partial_y \partial_x u_x = 0, \quad (58)$$

which guarantees a single-valued form of the in-plane displacement u_x , and thus absence of in-plane dislocations.

Based on the above discussion, we thus argue that at low temperature and weak disorder (certainly in the absence of point disorder, though it may even survive with weak point disorder [22]) the SmVG phase remains a dislocation-free, topologically ordered smectic Bragg glass [42].

V. SUMMARY AND CONCLUSIONS

Motivated by old experiments on vortex matter tilted away from columnar defects [39], in this paper we studied a new smectic glass state of vortex matter. We showed that it arises for large tilt angles of the magnetic field relative to columnar defects, at which a Bose glass undergoes a phase transition to this SmVG. As summarized in the Introduction, this novel state is characterized by a periodic translational

order along the columnar defects (exhibiting true Bragg peaks) and Bragg glass [19,22,42] logarithmically rough vortex distortions transverse to columnar defects, which lead to quasi-Bragg power-law peaks in the structure function. SmVG is also characterized by a divergent shear modulus in the plane transverse to the applied magnetic field, a counterpart of the “transverse” Meissner effect predicted for the Bose vortex glass [28,32]. We also predict that SmVG exhibits an infinite electrical transport anisotropy with a *nonzero* longitudinal resistivity transverse to columnar defects and to the applied magnetic field and a *vanishing* resistivity along the columnar defects.

In this paper, we focused on the purely transverse (tilt angle of $\pi/2$) geometry. However, based on the effective model and its symmetry (translational invariance along the columns), we expect the SmVG phase to exhibit a finite range of tilt angle stability. However, away from this purely transverse orientation, the symmetry of the state clearly changes from

biaxial to monoclinic. We leave the analysis of a more general geometry, as well as the nature of the Bose-to-smectic vortex glass phase transition, to future studies.

ACKNOWLEDGMENTS

It is a pleasure to thank Heinrich Jaeger and Tom Rosenbaum for sharing their data with me prior to publication and to acknowledge illuminating discussions with John Toner and Pierre Le Doussal. This research was supported by the Simons Investigator Award from the James Simons Foundation, and in part by the National Science Foundation through the Soft Materials Research Center under the NSF MRSEC Grant and through the KITP under Grant No. NSF PHY-1748958. I also thank the KITP for its hospitality during my stay as part of a sabbatical and the Synthetic Quantum Matter workshop, when part of this work was completed.

-
- [1] G. Blatter, M. V. Feigel'man, V. B. Geshkenbein, A. I. Larkin, and V. M. Vinokur, *Rev. Mod. Phys.* **66**, 1125 (1994).
- [2] T. Nattermann and S. Scheidl, *Adv. Phys.* **49**, 607 (2000).
- [3] D. S. Fisher, M. P. A. Fisher, and D. A. Huse, *Phys. Rev. B* **43**, 130 (1991).
- [4] D. A. Huse and L. Radzihovsky, in *Proceedings of 1993 Altenberg Summer School, Fundamental Problems in Statistical Mechanics VIII*, edited by H. van Beijeren and M. H. Ernst (Elsevier, Netherlands, 1993).
- [5] P. Le Doussal, *Int. J. Mod. Phys. B* **24**, 3855 (2010).
- [6] O. Narayan and D. S. Fisher, *Phys. Rev. B* **46**, 11520 (1992); A. E. Koshelev and V. M. Vinokur, *Phys. Rev. Lett.* **73**, 3580 (1994); T. Giamarchi and P. Le Doussal, *ibid.* **76**, 3408 (1996); P. Le Doussal and T. Giamarchi, *Phys. Rev. B* **57**, 11356 (1998); L. Balents, M. C. Marchetti, and L. Radzihovsky, *Phys. Rev. Lett.* **78**, 751 (1997); *Phys. Rev. B* **57**, 7705 (1998); S. Scheidl and V. M. Vinokur, *ibid.* **57**, 13800 (1998), and references therein.
- [7] M. Tinkham, *Introduction to Superconductivity* (Krieger Publishing Company, 1980).
- [8] G. Eilenberger, *Phys. Rev.* **164**, 628 (1967).
- [9] D. S. Fisher, *Phys. Rev. B* **22**, 1190 (1980).
- [10] D. R. Nelson, *Phys. Rev. Lett.* **60**, 1973 (1988); D. R. Nelson and S. Seung, *Phys. Rev. B* **39**, 9153 (1989).
- [11] P. L. Gammel, L. F. Scheemeyer, J. V. Waszczak, and D. J. Bishop, *Phys. Rev. Lett.* **61**, 1666 (1988); R. Cubitt, E. M. Forgan, G. Yang, S. L. Lee, D. M. Paul, H. A. Mook, M. Yethiraj, P. H. Kes, T. W. Li, A. A. Menovsky, Z. Tarnawski, and K. Mortensen, *Nature (London)* **365**, 407 (1993); E. Zeldov, D. Majer, M. Konczykowski, V. B. Geshkenbein *et al.*, *ibid.* **375**, 373 (1995); E. Zeldov *et al.*, *ibid.* **382**, 791 (1996).
- [12] A. Larkin, *Sov. Phys. JETP* **31**, 784 (1970); A. I. Larkin and Y. N. Ovchinnikov, *ibid.* **38**, 854 (1974).
- [13] Y. Imry and S. K. Ma, *Phys. Rev. Lett.* **35**, 1399 (1975).
- [14] R. H. Koch, V. Foglietti, W. J. Gallagher, G. Koren, A. Gupta, and M. P. A. Fisher, *Phys. Rev. Lett.* **63**, 1511 (1989).
- [15] M. P. A. Fisher, *Phys. Rev. Lett.* **62**, 1415 (1989).
- [16] J. L. Cardy and S. Ostlund, *Phys. Rev. B* **25**, 6899 (1982).
- [17] J. Toner and D. P. DiVincenzo, *Phys. Rev. B* **41**, 632 (1990).
- [18] S. F. Edwards and P. W. Anderson, *J. Phys. F* **5**, 4841 (1975).
- [19] T. Giamarchi and P. Le Doussal, *Phys. Rev. Lett.* **72**, 1530 (1994); *Phys. Rev. B* **52**, 1242 (1995).
- [20] D. Carpentier, P. Le Doussal, and T. Giamarchi, *Europhys. Lett.* **35**, 379 (1996).
- [21] J. Kierfeld, T. Nattermann, and T. Hwa, *Phys. Rev. B* **55**, 626 (1997).
- [22] D. S. Fisher, *Phys. Rev. Lett.* **78**, 1964 (1997).
- [23] M. J. P. Gingras and D. A. Huse, *Phys. Rev. B* **53**, 15193 (1996).
- [24] A. van Otterlo, R. T. Scalettar, and G. T. Zimanyi, *Phys. Rev. Lett.* **81**, 1497 (1998).
- [25] T. Klein, I. Joumard, S. Blanchard, J. Marcus, R. Cubitt, T. Giamarchi, and P. Le Doussal, *Nature (London)* **413**, 404 (2001).
- [26] L. Civale, A. D. Marwick, T. K. Worthington, M. A. Kirk, J. R. Thompson, L. Krusin-Elbaum, Y. Sum, J. R. Clem, and F. Holtzberg, *Phys. Rev. Lett.* **67**, 648 (1991).
- [27] M. P. A. Fisher and D. H. Lee, *Phys. Rev. B* **39**, 2756 (1989).
- [28] D. R. Nelson and V. M. Vinokur, *Phys. Rev. Lett.* **68**, 2398 (1992); *Phys. Rev. B* **48**, 13060 (1993).
- [29] M. P. A. Fisher, P. B. Weichman, G. Grinstein, and D. S. Fisher, *Phys. Rev. B* **40**, 546 (1989).
- [30] R. C. Budhani, M. Suenga, and S. H. Liou, *Phys. Rev. Lett.* **69**, 3816 (1992); W. Jiang, N.-C. Yeh, D. S. Reed, U. Kriplani, D. A. Beam, M. Konczykowski, T. A. Tombrello, and F. Holtzberg, *ibid.* **72**, 550 (1994); S. A. Grigera, E. Morr e, E. Osquiguil, C. Balseiro, G. Nieva, and F. de la Cruz, *ibid.* **81**, 2348 (1998).
- [31] J. Lidmar and M. Wallin, *Europhys. Lett.* **47**, 494 (1999).
- [32] L. Balents, *Europhys. Lett.* **24**, 489 (1993).
- [33] T. Hwa, D. R. Nelson, and V. M. Vinokur, *Phys. Rev. B* **48**, 1167 (1993).
- [34] B. I. Shklovskii and A. L. Efros, *Electronic Properties of Doped Semiconductors* (Springer, New York, 1984).

- [35] D. R. Nelson and L. Radzihovsky, *Phys. Rev. B* **54**, R6845 (1996).
- [36] W. Hofstetter, I. Affleck, D. R. Nelson, and U. Schollwöck, *Europhys. Lett.* **66**, 178 (2004); I. Affleck, W. Hofstetter, D. R. Nelson, and U. Schollwöck, *J. Stat. Mech.* (2004) P10003.
- [37] L. Radzihovsky, *Phys. Rev. B* **73**, 104504 (2006).
- [38] U. C. Tauber and D. R. Nelson, *Phys. Rep.* **289**, 157 (1997); C. Wengel and U. C. Tauber, *Phys. Rev. Lett.* **78**, 4845 (1997).
- [39] A. W. Smith, H. M. Jaeger, T. F. Rosenbaum, W. K. Kwok, and G. W. Crabtree, *Phys. Rev. B* **63**, 064514 (2001); A. W. Smith, H. M. Jaeger, T. F. Rosenbaum, A. M. Petrean, W. K. Kwok, and G. W. Crabtree, *Phys. Rev. Lett.* **84**, 4974 (2000).
- [40] Because the rotational invariance is *explicitly* broken by the columnar defects and the applied magnetic field, “smectic” vortex glass is not a “true” smectic controlled by the curvature elasticity. It thus does not exhibit the rich enhanced-fluctuation properties of a conventional liquid crystal smectic. It is, however, well characterized as a periodic array along a single (columnar) axis of vortex glass sheets with a vanishing inter-sheet shear modulus. Hence SmVG is a name that is (at least in part) appropriate.
- [41] D. S. Fisher, *Phys. Rev. B* **31**, 7233 (1985).
- [42] L. Radzihovsky and J. Toner, *Phys. Rev. B* **60**, 206 (1999).
- [43] E. H. Brandt and U. Essman, *Phys. Status Solidi B* **144**, 13 (1987); A. Houghton, R. A. Pelcovits, and A. Sudbo, *Phys. Rev. B* **40**, 6763 (1989); D. S. Fisher, in *Phenomenology and Applications of High-Temperature Superconductors*, edited by K. S. Bedell *et al.* (Addison-Wesley, 1992), p. 287.
- [44] Elastic moduli K and B can be derived from the Ginzburg-Landau theory and for finite-range interactions (set by the London penetration length λ) are wave vector dependent on scales shorter than λ , and become dispersionless only on scales longer than λ , i.e., for $n_0\lambda \ll 1$. For simplicity we will ignore this inessential complication.
- [45] In principle a more generic random stress disorder $\sigma_{ij}(\mathbf{x})\partial_i u_j = \mathbf{h}_x(\mathbf{x}) \cdot \nabla u_x + \mathbf{h}_z(\mathbf{x}) \cdot \nabla u_z$ will appear. We expect it to give additional, z -independent logarithmic contributions to vortex roughness, including in u_z . Because for weak disorder we expect these effects to be quantitatively weak and for the structure function to retain true Bragg peaks along the columnar defects (since all ground-state distortions are z independent), we will neglect these random stress contributions in the current work.
- [46] In the presence of columnar defects with transversely oriented vortex lattice, generically the elasticity will exhibit a biaxial (anisotropic C_2 symmetry) form, $H_{\text{el}} = \frac{1}{2} \int_{\mathbf{r}} [K_i (\partial_y u_i)^2 + c_{xx} u_{xx}^2 + c_{zz} u_{zz}^2 + c_{xz} u_{xx} u_{zz} + \mu_{zx} u_{xz}^2]$. However, because this does not introduce any new qualitative features but technically complicates the analysis, we will limit our treatment to isotropic elasticity, Eq. (7), except for the divergent shear modulus μ_{zx} induced by columnar disorder.
- [47] K. G. Wilson and J. Kogut, *Phys. Rep.* **12**, 75 (1974).